Accepted Manuscript

Title: PHOTODYNAMIC THERAPY PLATFORM BASED ON LOCALIZED DELIVERY OF PHOTOSENSITIZER BY VATERITE SUBMICRON PARTICLES

Author: Yu. I. Svenskaya A.M. Pavlov D.A. Gorin D.J. Gould B.V. Parakhonskiy G.B. Sukhorukov

PHOTODYNAMIC THERAPY PLATFORM BASED ON LOCALIZED DELIVERY OF PHOTOSENSITIZER BY VATERITE SUBMICRON PARTICLES

Yu. I. Svenskaya[1,2], A. M. Pavlov[1,2], D. A. Gorin[1,3], D. J. Gould[4], B. V. Parakhonskiy[1,5,6,*] and G. B. Sukhorukov[2,*]

1) Institute of Nanostructures and Biosystems, Saratov State University, 410012 Saratov, Russia.

2) School of Engineering and Materials Science, Queen Mary University of London, London, E1 4NS, United Kingdom.

3) Faculty of Nano- and Biomedical Technologies, Saratov State University, 410012, Saratov, Russia.

4) William Harvey Research Institute, Queen Mary University of London, London, EC1M 6BQ, United Kingdom.

5) A.V. Shubnikov Institute of Crystallography, RAS, 119333, Moscow, Russia.

6) Department of Molecular Biotechnology, Ghent University, 9000 Ghent, Belgium
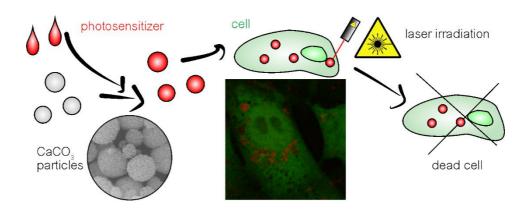
*Corresponding authors:

Bogdan Parakhonskiy, email: parbogd@crys.ras.ru,
Gleb Sukhorukov, email: g.sukhorukov@qmul.ac.uk.

Abstract

The elaboration of biocompatible and biodegradable carriers for photosensitizer targeted delivery is one of the most promising approaches in a modern photodynamic therapy (PDT). This approach is aimed at reducing sides effects connected with incidental toxicity in healthy tissue whilst also enhancing drug accumulation in the tumour area. In the present work, Photosens-loaded calcium carbonate ($CaCO_3$) submicron particles in vaterite modification are proposed as a novel platform for anticancer PDT. Fast penetration of the carriers (0.9 ± 0.2 μm in diameter) containing 0.12% (w/w) of the photosensitizer into NIH3T3/EGFP cells is demonstrated. The captured particles provide the dye localization inside the cell increasing its local concentration, compared with "free" Photosens solution which is uniformly distributed throughout the cell. The effect of photosensitizer encapsulation into vaterite submicron particles on cell viability under laser irradiation (670 nm, 19 mW/cm^2, 10 minutes) is discussed in the work. As determined by a viability assay, the encapsulation renders Photosens more phototoxic. By this means, $CaCO_3$ carriers allow improvement of the photosensitizer effectiveness supposing, therefore, the reduction of therapeutic dose. Summation of these effects with the simplicity, upscalability and cheapness of fabrication, biocompatibility and high payload ability of the vaterite particles hold out the prospect of a novel PDT platform.

Graphical abstract

Highlights

- Vaterite particles are prospective biocompatible carriers for PDT.
- The proposed carriers are capable of cellular uptake.
- Encapsulation increases local PS concentration inside cells improving phototoxicity.
- Vaterite particles encourage reduction of PS therapeutic dose.

1. Introduction

Among the clinical methods of cancer treatment, photodynamic therapy (PDT) is gaining much interest, since such externally activatable treatment modality allows the selective cell destruction in pathologic area sparing the normal tissue. [1,2] This therapy requires administration of a photosensitizing agent, followed by irradiation with light at the wavelength corresponding to absorption maximum of the agent. Activated photosensitizer transfers the energy to molecular oxygen resulting in the generation of reactive oxygen species and initiating a sequence of photochemical reactions, which cause death of cancer cells and tumour tissue destruction. [3,4] Although PDT has proven as an effective approach to cancer treatment and significantly improves the survival time for many patients, it still offers great potential for further improvement [2,5]. The development of novel carriers for targeted delivery of photosensitizers is one of the most promising approaches in a modern PDT. [6–9] This approach might overcome many side effects associated with classic photodynamic therapy, including an incidental toxicity in healthy tissue, might enhance the drug accumulation in the tumour area, and, by this means, might

improve the efficiency of the drug. Carriers such as liposomes [10–12], micelles [13,14], silica and calcium phosphate nanoparticles [15–17], quantum dots [18], polymeric and gold nanoparticles [19–21], have been previously applied for modification of various photosensitizers. Nevertheless, non-trivial storage conditions, instability, significant cytotoxicity and poor degradability, which are to different extents inherent to these materials, impede their application in biomedicine. Although a number of reports regard the inorganic nanomaterials with appropriate surface coatings as not notably toxic *in vitro* and *in vivo* in the tested dose ranges, it could still be extremely problematic for these agents to get FDA approval for clinical use. [1] The development of biocompatible and biodegradable carriers for anticancer PDT could thus be more clinically relevant.

Prospective matrices for such a delivery system are calcium carbonate particles (CaCO$_3$) in the form of vaterite, owing to its biocompatibility, large surface area and ability to decompose rapidly under mild conditions (pH below 6.5). [22–24] Such pH-sensitivity opens up new possibilities for targeted delivery, since the microenvironment in tumours is generally more acidic than in normal tissues. [25] High porosity of vaterite polycrystalline determines the high drug payload [26], that arouse interest toward the incorporation of various bioactive substances, like proteins [23,27,28], drugs [29,30] and DNA [31], into this matrix. By virtue of the fact, that vaterite is the least stable phase of calcium carbonate, and under the incubation in water-based solutions it gradually recrystallizes to stable calcite phase [32–34], such loaded particles release the drug without any external influence. Meanwhile, in the dried state the material shows high stability that enables long-term storage of the carriers at standard conditions. Biocompatibility tests for vaterite submicron-sized particles have demonstrated no indications of cytotoxicity and no influence on viability or metabolic activity *in vitro*. [35]

Hereby, CaCO$_3$ particle biodegradability, pH-sensitivity together with simplicity and cheapness of the fabrication technique hold out the prospect of its biomedical application, especially for novel PDT delivery system design. The additional tumour selectivity could be obtained through a particle surface modification, *e.g.* by attaching ligands interacting preferentially or specifically with tumour cells like monoclonal antibodies [36–38].

Previously, we have demonstrated the possibility of synthesizing micro- and submicron carriers for photosensitizer incorporation, whereupon we investigated the loading capacity of the carriers and a release mechanism depending on the surrounding pH. [24] However, efficiency of the treatment with such PDT containers still remains to be elucidated.

Thereby, in this work we focused on the investigation of cellular uptake, cytotoxicity and influence on cell viability of photosensitizer-loaded porous CaCO$_3$ submicron particles

in the absence and presence of light irradiation. To our knowledge, this is the first study dealing with an *in vitro* phototoxicity of photosensitizer-loaded vaterite carriers. These studies could enable their use in targeted cancer treatment with reduced therapeutic dose of the drug.

2. Experimental section

2.1 Materials

Calcium chloride ($CaCl_2$) and sodium carbonate (Na_2CO_3) were purchased from Sigma-Aldrich and used without further purification. Dulbecco's Modified Eagle Medium (DMEM) and phosphate-buffered saline (PBS), fetal bovine serum (FBS) and penicillin-streptomycin were purchased from Life Technologies. Thiazolyl blue tetrazolium bromide (MTT), and Igepal CA-630 were also purchased from Sigma-Aldrich.

The photosensitizer Photosens, a mixture of sulfonated aluminum phthalocyanines $AlPcS_n$, with n = 2, 3 or 4 (the mean n = 3.1), was obtained from the Organic Intermediates and Dyes Institute (Moscow, Russia). It has an absorption maximum at 675 nm wavelength and induces the photodynamic effect *in vivo* under irradiation by an appropriate laser with light doses of 100-250 J/cm^2. [39,40] The light doses of 1-15 J/cm^2 (depending on a Photosens concentration) can activate the phototoxic effect of Photosens *in vitro* [40,41] Photosens is a well-known drug applied in clinical practice since 2001 (Registration Certificate Ministry of Health of Russian Federation No 000199.01-2001) in both diagnostics and treatment. [42–46]

2.2 Container preparation and characterization

For preparation of calcium carbonate particles, 5-ml volumes of 1 M Na_2CO_3 and 1 M $CaCl_2$ water solutions were quickly added to 20 ml of deionized water in a glass vessel at room temperature and sonicated during 90 seconds by Ultrasonic Processor Gex-750 (Manufacturer) at a frequency of 20 kHz and radiation power of 75 W. The synthesized $CaCO_3$ particles were washed twice with water and once with ethanol and then freeze-dried. Photosens-loaded $CaCO_3$ particles were prepared by a co-precipitation method. [47] The same procedure as for pure $CaCO_3$ particles formation was used, with the only difference: 20 ml of 0.5 mg/ml Photosens solution was added instead of deionized water.

To study the morphology and microstructure, dried particles were sputtered with gold and imaged with a scanning electron microscope (SEM), a MIRA II LMU (Tescan) at acceleration voltage of 20 kV and a Phillips XL 30 at 5-30 kV.

Size distribution of particles was obtained by post processing and image analysis of SEM micrographs by Image J software (NIH, http://rsb.info.nih.gov/ij/). At least 4 overview SEM images per sample were used to collect 350 particle size measurements. The average size was shown as "mean ± standard deviation".

To study a crystallographic phase of pure and Photosens-loaded $CaCO_3$ particle, X-ray diffraction patterns of the powders were obtained on Xcalibur/Gemini and PDS120 (Nonius GmbH, Solingen) diffractometer using Cu-Ka radiation. The accelerating voltage and the applied current were 40 kV and 40 mA, respectively. The theoretical $CaCO_3$ spectra were taken from the works of Sitepu H. [48] and Le Bail A. [49] for calcite and vaterite, respectively.

In order to estimate the mass of Photosens loaded into $CaCO_3$ containers, their weighed portion was dissolved in aqueous solution of ethylenediaminetetracetic acid (EDTA, 0.2 M). As a measure of the amount of Photosens in solution, a fluorescence intensity was recorded at 684 nm by a Cary Eclipse fluorescence spectrometer (Varian) with excitation at 633 nm. A calibration curve was obtained from the measurements of known concentrations of Photosens in EDTA solution.

The loading capacity ($\%LC$) of containers was estimated according to equation:

$$\%LC = \frac{m_{Ph\ loaded}}{m_{particles}} \times 100\% \quad (1)$$

where $m_{Ph\ loaded}$ – the weight of Photosens incorporated into $CaCO_3$ particles, $m_{particles}$ – the weight of $CaCO_3$ particles.

2.3 Release and recrystallization process

To study the release of the drug, water and complete growth medium (DMEM supplemented with 10% inactivated FBS and 1% streptomycin–penicillin) were used. Vaterite containers loaded with Photosens were suspended in these solutions (6 mg of particles in 2 ml) and incubated at room temperature. After different incubation times (from 5 min to 7 days), the samples were centrifuged and the concentration of the released Photosens in the supernatant was measured by spectrofluorimetry using a Cary Eclipse fluorescence spectrometer (Varian). Then the measured solution was put back to the tube and incubated until the next measurement point. Calibration curves were obtained from the measurements of known concentrations of Photosens in both solution type (water and growth medium). To study the calcium carbonate phase change during

the release process, samples were monitored by SEM, to accomplish this 2 µl of particle suspension was collected and dried before the examination. The calcium carbonate phases were judged according to their appearance: spherical for the polycrystalline vaterite (Figure 1) and cubic for calcite monocrystal (Figure 2 b, c). After the last measurement, the sediment was dissolved in EDTA and the concentration of Photosens in the supernatant was also measured to calculate an amount of the drug that remained in the particles during the experiment.

2.4 Cell preparation and impregnation by containers

For cell experiments, green fluorescent Swiss albino mouse embryo tissue cells (NIH3T3/EGFP) were used. NIH3T3 cells were transduced with a lentivirus that encodes EGFP from an SFFV promoter. Cells were sorted by flow cytometry to select a population that highly expressed EGFP. NIH3T3/EGFP cells were cultured in Dulbecco's Modified Eagle Medium supplemented with 10% inactivated Fetal Bovine Serum, 1% streptomycin–penicillin and incubated at 37 °C under 5% CO_2 atmosphere. The pH of the growth medium was in its normal range (7.2-7.4). For the confocal fluorescence investigation, 2×10^5 cells per dish (3.5 cm^2 µDish, Ibidi) were incubated in 2 ml media overnight. For the cytotoxicity and viability assays, cells were seeded in a 96-multi well plate: 10^4 cells in 200 µl medium per well (0.32 cm^2) – and incubated overnight. Pure $CaCO_3$ particles, Photosens-loaded containers and Photosens solution were added then to cells and incubated for 24 hours. The concentration of added particles ($n_{particles\ added}$) was chosen based on the loaded drug amount ($m_{Ph\ loaded}$), as corresponding to the median lethal dose of Photosens solution ($LD50_{Ph}$=3 µg/ml). [50]

$$m_{Ph\ loaded} = LD50_{Ph} \times V \quad (2)$$

$$n_{particles\ added} = \frac{m_{particles\ added}}{V} = \frac{LD50_{Ph}}{\%LC} \times 100\% \quad (3)$$

where V – the volume of medium added to the cells, $m_{particles\ added}$ – the weight of particles added to the cells calculated relying on equations (1) and (2).

Hence, the concentration of $CaCO_3$ particles added to the cells amounted to 0.25 mg/ml. Such concentration of the particles didn't affect the pH of the growing media, assuming the colour of the media containing a phenol red indicator dye.

2.5 Cellular uptake investigation

To visualize viable cells and evaluate container uptake, a confocal laser scanning microscope Leica TCS SP5 (Leica, Germany) was used. After 24 hours of incubation with Photosens-loaded

CaCO$_3$ containers and Photosens solution, cell cultures were rinsed 3 times with PBS to remove free particles and free photosensitizer and thereafter were returned to growth medium. Confocal fluorescent images and Z-sequences of optical slices (3D image reconstruction) were obtained. To visualize viable fluorescent NIH3T3 cells and the photosensitizer inside, 488-nm and 633-nm lasers were used together: first one at 10% of its power to excite EGFP, expressed by cells, and the second one – at 15% to excite the fluorescence of Photosens.

2.6 Fluorescence investigation of cell viability under the laser irradiation

To visualize an effect of laser irradiation on NIH3T3/EGFP cells impregnated with pure and Photosens-loaded CaCO$_3$ containers and Photosens solution, confocal laser scanning microscopy was applied. The control samples with NIH3T3/EGFP cells, incubated without any modifications, were also investigated.

The cells were irradiated by Collimated Laser Diode CPS186 (Throlabs) at 670 nm with the power density of 19 mW/cm^2 during 10 minutes meaning the light dose of 11.4 J/cm^2. The beam cross-section area was set at 0.32 cm^2 and the irradiated area was marked at the dish bottom. As far as the light doses of 6-12 J/cm^2 do not induce intracellular ROS generation for NIH3T3 cells [51], the usage of such irradiation parameters should enable integrity of cells exposed to the light in absence of the photosensitizer allowing separation of the drug effect and exclusion of the laser damaging effect itself.

All samples were visualized before and immediately after the irradiation using a confocal laser scanning microscope Leica TCS SP5 (Leica, Germany) at the same scanning parameters, as the cellular uptake investigation.

2.7 Cytotoxicity assay

For the cytotoxicity investigation the colorimetric MTT (3-(4-5-dimethylthiazol-2-yl)-2,5-diphenyltetrazolium bromide) assay [52] was used. Briefly, NIH3T3/EGFP cells were seeded in a 96-multi well plate and incubated with pure and Photosens-loaded submicron containers and Photosens solution as it was described above. Control wells inoculated with the cells were cultivated without any treatment. After 24 hours of incubation at 37 °C under 5% CO$_2$ atmosphere with containers and solutions, cell layers were rinsed 3 times with PBS and incubated in growth medium. Half of the 96-multi well plate was irradiated well-by-well by the laser using the parameters described above (paragraph 2.6), thereupon the plate was incubated overnight at 37˚C under 5% CO$_2$ and the toxicity test was carried out according to MTT protocol. Wherein, MTT powder was dissolved in PBS at a concentration of 5 mg/ml, the solution was subsequently filter-

sterilized. Twenty microliters of the solution were added to each well, including blank wells with no cells. After 3.5 hours of incubation, the media was carefully removed and 150 µl of Igepal CA-630 0.1% in 4 mM hydrochloric acid was added to the wells. Thereafter, the plate was covered with tinfoil and agitated on a shaker for 15 min. The absorbance was read at 590 nm by means of Multiskan Ascent 96/384 Plate Reader (MTX Lab Systems Inc., USA). The average absorbance of the blank wells, in which cells were omitted, was subtracted from the readings of the other wells. The average absorbance of the control untreated NIH3T3/EGFP cells, represented 100% cell survival. The relative cell viability (%) related to control cells was shown as "mean ± standard deviation' of n=5 independent determinations.

Statistical analysis was performed by one-way ANOVA on n = 5 independent samples followed by Tukey post-hoc test, significance was assigned at p-values <0.05. Equality of variances was checked using the F-test with a significant level of 0.05.

3. Results and discussions

3.1 Preparation of Photosens-loaded particles

The wet synthesis of polycrystalline spherical vaterite particles under ultrasound (US) was applied [53]. This method is based on US-accomplished precipitation of $CaCO_3$ from the saturated solutions of $CaCl_2$ and Na_2CO_3 and allows the formation of porous particles with low dispersity, as far as ultrasonic field influences on crystallization process by enhancing the primary nucleation and preventing the agglomeration. In addition, this preparation technique was proven to be upscalable by virtue of the fact, that increment of the reaction volume enhanced the particle reaction yield without any significant losses in the sample quality [53].

The SEM image of obtained $CaCO_3$ particles, presented in Figure 1 (a), demonstrates a spherical shape of the particles with an average size of 0.9±0.2 µm. Size distribution histogram is presented in Figure S1 (a) (see Supplementary Information).
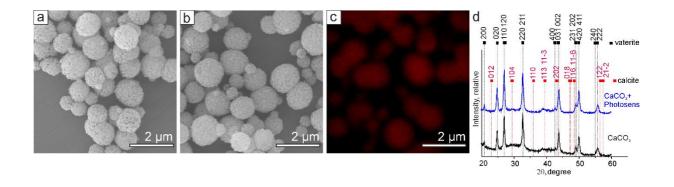
Figure 1. Scanning electron microscopy images of pure (a) and Photosens-loaded (b) $CaCO_3$ particles, confocal fluorescent image of Photosens-loaded $CaCO_3$ particles (c) and XRD data of pure (black curve in d) and Photosens-loaded $CaCO_3$ particles (blue curve in d), where red squares and numbers correspond to calcite peaks and miller indexes, black squares and numbers correspond to vaterite ones.

A spherical shape of the particles indicates the vaterite phase of $CaCO_3$, that was proved out by the XRD data presented in Figure 1d. The XRD pattern of pure $CaCO_3$ particles (black curve in Figure 1d) exhibits the characteristic reflection for vaterite owning to the peaks corresponding to 020, 110, 120, 220, 211 planes (black squares and numbers in Figure 1d). The peaks, which are typical for calcite phase of $CaCO_3$ (red squares and numbers in Figure 1d), were not observed on the XRD pattern.

Photosensitizer-loaded $CaCO_3$ particles were prepared by the US-assisted co-precipitation method. In the co-precipitation technique, the drug is added to the reaction solution during calcium carbonate synthesis resulting in its entrapment into the structure of formed particles. In comparison with the physical adsorption technique, where the active substance should be adsorbed from the solution onto preformed particles, this method allows one to encapsulate five times higher amounts of biologically active substance. [47] Photosens (sulfonated aluminum phthalocyanine) was used as a photosensitizer, whereas this anticancer drug has been successfully applied in clinical practice since 2001 in both diagnostics and treatment. [42–46]

The SEM and confocal fluorescent images of loaded containers (Figure 1 b, c) demonstrate the spherical shape of vaterite polycrystal particles with a size of 0.9±0.2 μm (size distribution histogram is presented in Figure S1b in Supplementary Information). The fluorescence signal from confocal microscopy in Figure 1 (c) demonstrated, that particles were successfully loaded with Photosens, preserving its fluorescence properties. As estimated by the spectrofluometric method, the loading capacity of containers corresponded to 0.12 % (w/w), that means 6 μg of Photosens incorporated to 5 mg of $CaCO_3$ particles. The diffraction data for Photosens-loaded particles (blue curve in Figure 1d) demonstrate the presence of only vaterite phase, meaning that the addition of photosensitizer to the reaction mixture has no significant influence on crystallization process.

3.2 Photosens release process

Subsequently, release kinetic of Photosens from the containers was studied in water and in complete cell culture medium.

As demonstrated previously [24,54,55], the release of the payload from the porous calcium carbonate particles is an interplay of drug desorption and carrier recrystallization. Being the least stable phase of $CaCO_3$, vaterite slowly dissolves and recrystallizes to calcite form in contact with water, releasing the payload. Depending on the immersion medium, the vaterite particles dissolve or a crystal phase transition sets in, where the external layer of particles starts to ionize, seeding the formation of calcite monocrystals from the ions. The release curves of Photosens from containers were monitored via spectrofluorimetry and the corresponding calcium carbonate crystal phases were investigated via SEM for both immersion mediums.

Observations started 5 min (0.83 hours) after immersion and lasted up to 7 days (168 hours). The main results, presented in SEM images (Figure 2), were found to be in good agreement with the release data, demonstrated in Figure 3.
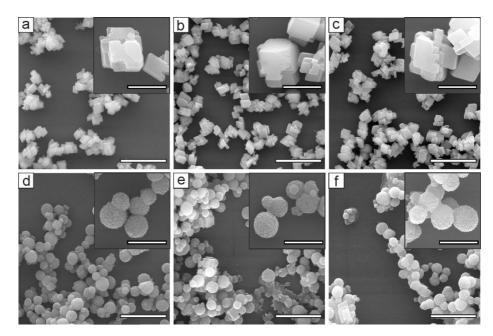

Figure 2. Scanning electron microscopy images of Photosens-loaded $CaCO_3$ particles at different incubation time in water (top line a-c) and in cell medium (bottom line d-f): a, d – 24 hours, b, e – 48 hours, c, f – 168 hours. The scale bars on main scans and insets for the top row of images correspond to 20 μm and to 5 μm, respectively; and to 5 μm and 2 μm for the bottom row.
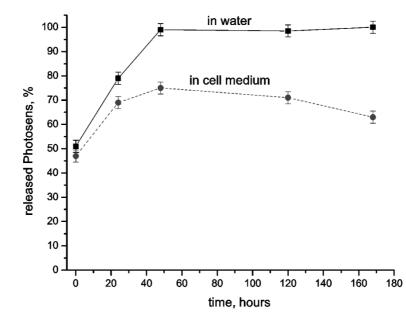
Figure 3. Release profiles of Photosens from porous CaCO$_3$ submicron containers immersed in water and in cell medium during 7 days. The error bars represent standard error of the mean of release measurements for n=3 independent samples.

The release of Photosens from the carriers is defined by desorption in the initial phase of incubation (during 5 minutes) and was followed by release during the recrystallization. Being immersed in either water or cell medium, CaCO$_3$ particles released around 50% of loaded Photosens within 5 minutes (Figure 3) by desorption from the exterior particle surface. As a prevention of the premature payload release, a particle covering with a polyelectrolyte layer (polyethylene glycol *e.g.*) can be used when required [56]. Such a polymer deposition could inhibit the desorption of drug molecules without affecting the recrystallization kinetics of CaCO$_3$ [57].

Fast recrystallization of CaCO$_3$ containers from vaterite to calcite took place, while incubating in water. The transition sets in at around 24 hours (Figure 2 a), and correlates with previously reported results. [24] The external layer of particles was recrystallized to calcite, meanwhile for the inner part the process continued. The transition was completed after 48 hours of incubation, reflecting in 100% release of loaded Photosens during the formation of smooth calcite crystals (Figure 2b and Figure 3).

In the cell medium the highest released percent of loaded Photosens (70±5%) was observed on the second day of incubation (Figure 3), when a small amount of cubic-like particles occurred (Figure 2 e). During 1 week of incubation in the cell medium the vaterite-calcite recrystallization was not completed and the amount of cubic-like particles remained negligible (Figure 2f). This was reflected in the payload release profile (Figure 3): decreasing of released Photosens amount up to 62±5 % was observed, due to re-adsorption of Photosens molecules back on the surface of CaCO$_3$ particles.

Such delay of the recrystallization can be explained by the adsorption of proteins from the cell medium on the surface of $CaCO_3$ carriers. A similar effect, called "corona", was previously observed for different container types while its incubation in model solutions contained proteins. [58–60] The protein molecules stabilize the particle surface, and prevent recrystallization reflected as a slowdown of payload release.

The prolongation of drug release from the vaterite submicron carriers can be considered as a beneficial advantage of the proposed system for *in vivo* application allowing the reduction of the payload loss in biological fluids (plasma, or otherwise), associated with the "protein corona" organized by biopolymers from the fluid. By this means, the drug release could be postponed up to the moment of delivery at the right site of action. Furthermore, this "protein corona" effect offers a novel strategy for targeted drug delivery owing to the modification of particle surface by specific proteins, which could provide its transportation and efficient cell internalization. [61]

3.3 Cellular uptake

For *in vitro* investigation of container uptake, cytotoxicity and phototoxicity, green fluorescent NIH3T3/EGFP cells were used. The median lethal dose (LD50) of Photosens (3 μg/ml) [50] was added to the cells both, in free and immobilized form into $CaCO_3$ particles, in order to investigate an effect of photosensitizer encapsulation.

The uptake process analysis was performed by confocal laser scanning microscopy and the images are represented in Figure 4.
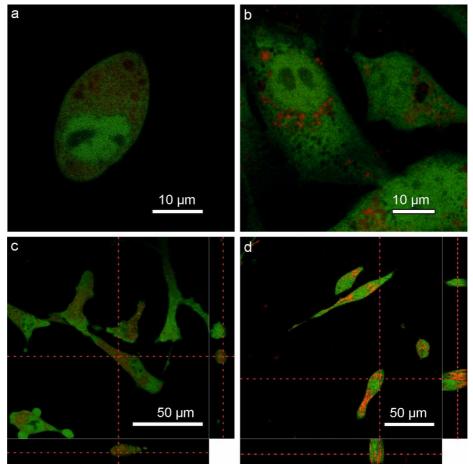
Figure 4. Fluorescent confocal images, including 3D reconstruction (c, d), of NIH3T3/EGFP cells after 24 hours of incubation with Photosens solution (a, c) and with Photosens-loaded $CaCO_3$ particles (b, d).

3D stacks of fluorescent images (Figure 4 c, d) demonstrated that the photosensitizer was uniformly distributed inside the cells (Figure 4 c) or was localized also inside the carriers trapped by cells (bright red spots within the cells at Figure 4 d). Thus, $CaCO_3$ particles loaded with Photosens and captured by cells provided dye localization inside the cell increasing its local concentration, compared with "free" Photosens solution. The uptake within 24 hours was found to be equal to 44 ± 5 containers per cell.

In order to evaluate the amount of Photosens, which had been trapped by cells within 24 hours, and the percentage in spread and localized state, the supernatant from the cells after the container incubation was collected for fluorometric investigation. Subsequent analysis of the data and calculations (see Supplementary Information) have established, that 85% of added 'free' Photosens was entrapped by cells, compared to 53% with Photosens-loaded particles. According to the Photosens release profile (Figure 3, 24 hours in cell medium), 70% of the amount loaded into $CaCO_3$ particles was released by that time.

Taking that loss into account, we estimated the possible range of captured amount of Photosens localized inside the containers while delivered into cells in the time course.

The lower value of estimated drug amount ($m_{min\ Ph\ entrapped\ loc}$) reflects the instantaneous cellular uptake of the particles containing 30% of loaded photosensitizer as particles release the drug before uptake:

$$m_{min\ Ph\ entrapped\ loc} = 0.3 \times \frac{\%LC}{100\%} \times m_{particles\ entrapped} \quad (4)$$

where $m_{particles\ entrapped}$ – the mass of Photoses-loaded CaCO$_3$ particles entrapped by cells during 24 hours (see Supplementary Information).

Whereas the upper estimation ($m_{max\ Ph\ entrapped\ loc}$) considers no release of the drug before the uptake and hence the 100%-loading of captured containers:

$$m_{max\ Ph\ entrapped\ loc} = \frac{\%LC}{100\%} \times m_{particles\ entrapped} \quad (5)$$

This means, 5-18% of the photosensitizer remained inside the CaCO$_3$ particles after 24-hours uptake by cells, while the rest of the entrapped Photosens had been released from the containers and subsequently spread inside the cell interior.

3.4 Cellular phototoxicity under the laser irradiation: fluorescence investigation and toxicity assay

Photosens-loaded and pure CaCO$_3$ particles, as well as "free" Photosens solution, were incubated with NIH3T3/EGFP cells for 24 hours. Then cells were carefully washed and irradiated by the laser with a wavelength corresponding to the Photosens adsorption maximum (670 nm) for 10 minutes. The effect of laser irradiation on cells was investigated by confocal laser scanning microscopy before and after the irradiation (Figure 5) and estimated by MTT assay (Figure 6).
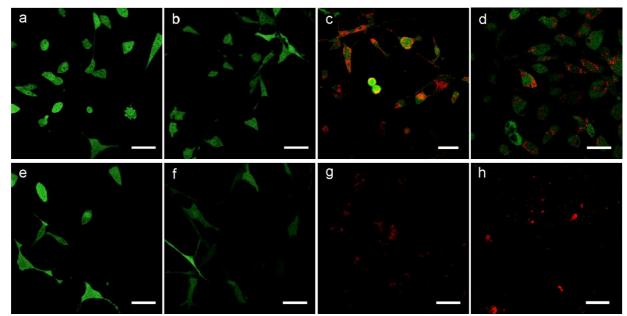
Figure 5. Confocal fluorescent images of NIH3T3/EGFP cells before (a-d) and after irradiation (e-h): control cells (a, e), cells impregnated with pure (b, f) and Photosens-loaded (c, g) $CaCO_3$ particles, cells cultured with Photosens solution (d, h). The scale bar is equal to 50 μm
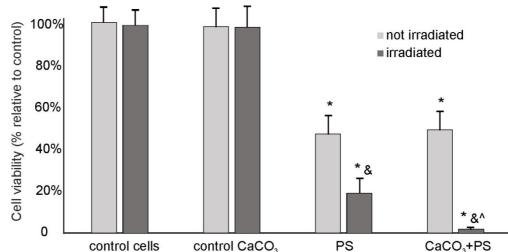

Figure 6. Cytotoxic effect of calcium carbonate particles (control $CaCO_3$), "free" Photosens solution (PS) and Photosen-loaded $CaCO_3$ particles ($CaCO_3$+PS) on NIH3T3/EGFP cells without (light grey columns) and with (dark grey columns) laser irradiation. The concentration of pure and loaded $CaCO_3$ particles was 0.25 mg/ml, the corresponding Photosens concentration was 3 μg/ml. The cell viability was determined by MTT metabolism assay and shown as "mean ± standard deviation" of n=5 independent determinations. An asterisk (*) indicates significant differences from the control cell group. An ampersand (&) denotes significant differences between irradiated and not irradiated samples containing Photosens. A caret (^) indicates a significant difference in cell viability under the irradiation between the samples pretreated with encapsulated and "free" Photosens forms. The statistical analysis was performed by ANOVA followed by the Tukey test (P<0.05)).

As was reported before, the death of EGFP expressing cells could be observed by the decrease of their fluorescence. [62] Thereby, the fluorescence investigation of NIH3T3/EGFP before and after the laser irradiation allows the visualization of an effect of this irradiation: the bright green signal images only the cells, which are alive and maintain EGFP expression, meanwhile dead cells have no fluorescence in a green channel.

Comparison of the fluorescence of "control" cells and cells treated with pure $CaCO_3$ particles before (Figure 5 a, b) and after irradiation (Figure 5 e, f) demonstrated, that the application of $CaCO_3$ particles, even at a high concentration (1 mg/cm^2 of dish surface), as well, as laser irradiation, didn't affect cell viability in the absence of photosensitizer. This effect was borne out by the MTT assay which demonstrated a high average survival rate of NIH3T3/EGFP cells (Figure 6).

The uptake of Photosens in "free" form (Figure 5 d, h) and immobilized into $CaCO_3$ particles (Figure 5 c, g) by NIH3T3/EGFP cells caused the loss of the fluorescent signal in a green channel under laser irradiation. The red spots on these confocal images denote the fluorescent signal in a red channel from the entrapped Photosens and therefore indicate the presence of the cells in the field of view. The overlay of both fluorescent channels allowed the distinction between alive (Figure 5 c, d) and dead (Figure 5 g, h) NIH3T3/EGFP cells, and by this means illustrated a phototoxic effect for both, Photosens solution and Photosens immobilized into $CaCO_3$ particles.

Significant phototoxic effect was also demonstrated using the MTT assay for immobilized and free Photosens (Figure 6). A drastic difference in the percentage of viable cells was observed: 2% versus 20%, correspondently. Moreover, the release investigation demonstrated, that by the time of irradiation a higher photosensitizer amount had been entrapped by NIH3T3/EGFP cells from Photosens solution (85%), than from Photosens-loaded particles (53%). By this means, $CaCO_3$ particles loaded with Photosens proved to be almost 20-times more effective compared to "free" Photosens solution. Increasing the local concentration of a drug inside the cell, $CaCO_3$ particles are capable of decreasing its concentration in the system, and therefore, potentially allow the reduction of therapeutic dose.

4. Conclusions

In the current work, we have proposed a novel platform for anticancer PDT. The platform is based on Photosens-loaded calcium carbonate submicron particles fabricated by ultrasound-assisted co-precipitation method. By virtue of the demonstration, the photosensitizer release from the carriers arises mostly from the vaterite-calcite recrystallization of $CaCO_3$. Sustained release has been achieved by suppression of recrystallization as a result of particle surface stabilization with proteins from the cell medium. Such effect holds out the prospect of *in vivo* application of the proposed system, since it allows a reduction of the payload loss in biological fluids, associated with the "protein corona" organized by biopolymers from the fluid. The cellular uptake experiments

have demonstrated fast penetration of the Photosens-loaded particles into NIH3T3/EGFP cells. The captured carriers have provided dye localization inside cells increasing its local concentration compared with delivery from "free" Photosens solution uniformly distributed throughout the cell. Significant phototoxic effect was discovered for both, Photosens solution and for $CaCO_3$ particles loaded with Photosens, meanwhile the irradiation alone had no influence on cell viability in the absence of the photosensitizer. The biocompatibility of pure $CaCO_3$ particles was demonstrated, since they did not influence cell viability. According to MTT results, $CaCO_3$ particles loaded with Photosen were almost 20-times more effective compared to "free" Photosens solution at killing cells. Improving the drug effectiveness, $CaCO_3$ particles potentially support the reduction of its therapeutic dose. This effect has revealed the promising outlook of the proposed system for application in PDT, as well as in nanomedicine in general, since it might overcome non-specific toxicity in healthy tissue caused by using a high dose. At the same time, simplicity, upscalability and cheapness of the fabrication, biocompatibility and high payload ability of the vaterite particles open up perspectives beyond the scope of cancer treatment.

Supplementary information

Size distribution histograms of pure and Photosens-loaded $CaCO_3$ particles obtained by image analysis of SEM micrographs are presented in Figure S1 in Supplementary Information.

Subsequent calculations of the Photosens amount, which had been entrapped by cells within 24 hours, and its percentage in spread and localized state are also presented in Supplementary Information.

References

[1]   L. Cheng, C. Wang, L. Feng, K. Yang, Z. Liu, Functional nanomaterials for phototherapies of cancer., Chem. Rev. 114 (2014) 10869–939.

[2]   T.J. Dougherty, C.J. Gomer, B.W. Henderson, G. Jori, D. Kessel, M. Korbelik, et al., Photodynamic Therapy, JNCI J. Natl. Cancer Inst. 90 (1998) 889–905.

[3]   M. DeRosa, R. Crutchley, Photosensitized singlet oxygen and its applications, Coord. Chem. Rev. 233-234 (2002) 351–371.

[4]   T.J. Dougherty, J.E. Kaufman, A. Goldfarb, K.R. Weishaupt, D. Boyle, A. Mittleman, Photoradiation therapy for the treatment of malignant tumors, Cancer Res. 38 (1978) 2628–2635.

[5]   R.R. Allison, C.H. Sibata, Oncologic photodynamic therapy photosensitizers: A clinical review, Photodiagnosis Photodyn. Ther. 7 (2010) 61–75.

[6]   E. Paszko, C. Ehrhardt, M.O. Senge, D.P. Kelleher, J. V Reynolds, Nanodrug applications in photodynamic therapy., Photodiagnosis Photodyn. Ther. 8 (2011) 14–29.

[7]   D.K. Chatterjee, L.S. Fong, Y. Zhang, Nanoparticles in photodynamic therapy: an emerging paradigm., Adv. Drug Deliv. Rev. 60 (2008) 1627–37.

[8]   R.R. Allison, Future PDT., Photodiagnosis Photodyn. Ther. 6 (2009) 231–4.

[9]   Y. Han, J. Bu, Y. Zhang, W. Tong, C. Gao, Encapsulation of Photosensitizer into Multilayer Microcapsules by Combination of Spontaneous Deposition and Heat-Induced Shrinkage for Photodynamic Therapy, Macromol. Biosci. 12 (2012) 1436–1442.

[10]   A.S.L. Derycke, P.A.M. De Witte, Liposomes for photodynamic therapy, Adv. Drug Deliv. Rev. 56 (2004) 17–30.

[11]   M.A. Kortava, A. V. Ryabova, E. V. Ignatyeva, A.P. Polozkova, O.L. Orlova, A.A. Stratonnikov, et al., The investigation of photosense efficient inclusion into sterically stabilized liposomes, Russ. Biother. J. 4 (2005) 96–101.

[12]   F. Jiang, L. Lilge, J. Grenier, Y. Li, M.D. Wilson, M. Chopp, Photodynamic therapy of U87 human glioma in nude rat using liposome-delivered photofrin, Lasers Surg. Med. 22 (1998) 74–80.

[13]   C.F. van Nostrum, Polymeric micelles to deliver photosensitizers for photodynamic therapy, Adv. Drug Deliv. Rev. 56 (2004) 9–16.

[14] N. Nishiyama, Y. Morimoto, W.-D. Jang, K. Kataoka, Design and development of dendrimer photosensitizer-incorporated polymeric micelles for enhanced photodynamic therapy, Adv. Drug Deliv. Rev. 61 (2009) 327–338.

[15] J. Qian, D. Wang, F. Cai, Q. Zhan, Y. Wang, S. He, Photosensitizer encapsulated organically modified silica nanoparticles for direct two-photon photodynamic therapy and In Vivo functional imaging, Biomaterials. 33 (2012) 4851–4860.

[16] H.-L. Tu, Y.-S. Lin, H.-Y. Lin, Y. Hung, L.-W. Lo, Y.-F. Chen, et al., In vitro Studies of Functionalized Mesoporous Silica Nanoparticles for Photodynamic Therapy, Adv. Mater. 21 (2009) 172–177.

[17] J. Schwiertz, A. Wiehe, S. Gräfe, B. Gitter, M. Epple, Calcium phosphate nanoparticles as efficient carriers for photodynamic therapy against cells and bacteria, Biomaterials. 30 (2009) 3324–3331.

[18] A.C.S. Samia, X. Chen, C. Burda, Semiconductor quantum dots for photodynamic therapy., J. Am. Chem. Soc. 125 (2003) 15736–7.

[19] E. Ricci-Júnior, J.M. Marchetti, Zinc(II) phthalocyanine loaded PLGA nanoparticles for photodynamic therapy use., Int. J. Pharm. 310 (2006) 187–95.

[20] K.J. Son, H.-J. Yoon, J.-H. Kim, W.-D. Jang, Y. Lee, W.-G. Koh, Photosensitizing Hollow Nanocapsules for Combination Cancer Therapy, Angew. Chemie Int. Ed. 50 (2011) 11968–11971.

[21] H. Eshghi, A. Sazgarnia, M. Rahimizadeh, N. Attaran, M. Bakavoli, S. Soudmand, Protoporphyrin IX–gold nanoparticle conjugates as an efficient photosensitizer in cervical cancer therapy, Photodiagnosis Photodyn. Ther. 10 (2013) 304–312.

[22] D.B. Trushina, T. V. Bukreeva, M. V. Kovalchuk, M.N. Antipina, CaCO3 vaterite microparticles for biomedical and personal care applications, Mater. Sci. Eng. C. (2014).

[23] D. V. Volodkin, R. von Klitzing, H. Möhwald, Pure protein microspheres by calcium carbonate templating, Angew. Chem. Int. Ed. Engl. 49 (2010) 9258–61.

[24] Y. Svenskaya, B. Parakhonskiy, A. Haase, V. Atkin, E. Lukyanets, D. Gorin, et al., Anticancer drug delivery system based on calcium carbonate particles loaded with a photosensitizer., Biophys. Chem. 182 (2013) 11–15.

[25] I. Tannock, D. Rotin, Acid pH in tumors and its potential for therapeutic exploitation, Cancer Res. (1989) 4373–4384.

[26] D. V. Volodkin, A.I. Petrov, M. Prevot, G.B. Sukhorukov, Matrix Polyelectrolyte Microcapsules: New System for Macromolecule Encapsulation, Langmuir. 20 (2004) 3398–3406.

[27] M. Fujiwara, K. Shiokawa, K. Morigaki, Y. Zhu, Y. Nakahara, Calcium carbonate microcapsules encapsulating biomacromolecules, Chem. Eng. J. 137 (2008) 14–22.

[28] T. Borodina, L. Rumsh, Polyelectrolyte microcapsules as the systems for delivery of biologically active substances, Biochem. Suppl. Ser. B Biomed. Chem. 2 (2008) 88–93.

[29] C. Peng, Q. Zhao, C. Gao, Sustained delivery of doxorubicin by porous CaCO3 and chitosan/alginate multilayers-coated CaCO3 microparticles, Colloids Surfaces A Physicochem. Eng. Asp. 353 (2010) 132–139.

[30] C. Wang, C. He, Z. Tong, X. Liu, B. Ren, F. Zeng, Combination of adsorption by porous CaCO3 microparticles and encapsulation by polyelectrolyte multilayer films for sustained drug delivery, Int. J. Pharm. 308 (2006) 160–7.

[31] T. Borodina, E. Markvicheva, S. Kunizhev, H. Möhwald, G.B. Sukhorukov, O. Kreft, Controlled Release of DNA from Self-Degrading Microcapsules, Macromol. Rapid Commun. 28 (2007) 1894–1899.

[32] J.-Y. Gal, J.-C. Bollinger, H. Tolosa, N. Gache, Calcium carbonate solubility: a reappraisal of scale formation and inhibition, Talanta. 43 (1996) 1497–1509.

[33] D. Kralj, L. Brečević, A. Nielsen, Vaterite growth and dissolution in aqueous solution II. Kinetics of dissolution, J. Cryst. Growth. 143 (1994) 269–276.

[34] D. Kralj, L. Brečević, J. Kontrec, Vaterite growth and dissolution in aqueous solution III. Kinetics of transformation, J. Cryst. Growth. 177 (1997) 248–257.

[35] B. V Parakhonskiy, C. Foss, E. Carletti, M. Fedel, A. Haase, A. Motta, et al., Tailored intracellular delivery via a crystal phase transition in 400 nm vaterite particles, Biomater. Sci. 1 (2013) 1273.

[36] S.K. Kim, M.B. Foote, L. Huang, Targeted delivery of EV peptide to tumor cell cytoplasm using lipid coated calcium carbonate nanoparticles., Cancer Lett. 334 (2013) 311–8.

[37] B.G. De Geest, S. De Koker, G.B. Sukhorukov, O. Kreft, W.J. Parak, A.G. Skirtach, et al., Polyelectrolyte microcapsules for biomedical applications, Soft Matter. 5 (2009) 282–291.

[38] J. Wei, T. Cheang, B. Tang, H. Xia, Z. Xing, Z. Chen, et al., The inhibition of human bladder

cancer growth by calcium carbonate/CaIP6 nanocomposite particles delivering AIB1 siRNA, Biomaterials. 34 (2013) 1246–1254.

[39]   R.R. Allison, G.H. Downie, R. Cuenca, X.-H. Hu, C.J. Childs, C.H. Sibata, Photosensitizers in clinical PDT, Photodiagnosis Photodyn. Ther. 1 (2004) 27–42.

[40]   I.G. Meerovich, V. V. Jerdeva, V.M. Derkacheva, G.A. Meerovich, E.A. Lukyanets, E.A. Kogan, et al., Photodynamic activity of dibiotinylated aluminum sulfophthalocyanine in vitro and in vivo, J. Photochem. Photobiol. B Biol. 80 (2005) 57–64.

[41]   W.S. Chan, C.M. West, J. V Moore, I.R. Hart, Photocytotoxic efficacy of sulphonated species of aluminium phthalocyanine against cell monolayers, multicellular spheroids and in vivo tumours, Br. J. Cancer. 64 (1991) 827–832.

[42]   S.A. Shevchik, M. V Loshchenov, G.A. Meerovich, M. V Budzinskaia, N.A. Ermakova, S.S. Kharnas, et al., A device for fluorescence diagnosis and photodynamic therapy of eye diseases, by using photosense., Vestn. Oftalmol. 121 (2005) 26–28.

[43]   M. V Budzinskaia, S.A. Shevchik, T.N. Kiseleva, V.B. Loshchenov, I. V Gurova, I. V Shchegoleva, et al., Role of fluorescence diagnosis using Photosens in patients with subretinal neovascular membrane., Vestn. Oftalmol. 123 (2007) 11–6.

[44]   E. V. Filonenko, V. V. Sokolov, V.I. Chissov, E.A. Lukyanets, G.N. Vorozhtsov, Photodynamic therapy of early esophageal cancer., Photodiagnosis Photodyn. Ther. 5 (2008) 187–90.

[45]   O.I. Trushina, E.G. Novikova, V. V. Sokolov, E. V. Filonenko, V.I. Chissov, G.N. Vorozhtsov, Photodynamic therapy of virus-associated precancer and early stages cancer of cervix uteri., Photodiagnosis Photodyn. Ther. 5 (2008) 256–9.

[46]   O.I. Apolikhin, I. V. Chernishov, A. V. Sivkov, D. V. Altunin, S.G. Kuzmin, G.N. Vorozhtsov, Adjuvant photodynamic therapy (PDT) with photosensitizer photosens for superficial bladder cancer: experimental investigations to treat prostate cancer by PDT with photosens, in: A. Vogel (Ed.), Prog. Biomed. Opt. Imaging, Society of Photo-Optical Instrumentation Engineers, 2007: p. 663213.

[47]   A.I. Petrov, D. V. Volodkin, G.B. Sukhorukov, Protein-calcium carbonate coprecipitation: a tool for protein encapsulation., Biotechnol. Prog. 21 (2005) 918–25.

[48]   H. Sitepu, Texture and structural refinement using neutron diffraction data from molybdite (MoO3) and calcite (CaCO3) powders and a Ni-rich Ni50.7Ti49.30 alloy, Powder Diffr. 24

(2009) 315–326.

[49]   A. Le Bail, S. Ouhenia, D. Chateigner, Microtwinning hypothesis for a more ordered vaterite model, Powder Diffr. 26 (2012) 16–21.

[50]   I.M. Parkhomenko, A.P. Zarubina, E.P. Lukashev, E.F. Stranadko, K.N. Timofeev, A.B. Rubin, On the Mechanisms of Photodynamic Effect of Sensitizers and Improvement of Methods of Their Primary Selection for Photodynamic Antimicrobial Therapy, Dokl. Biochem. Biophys. 404 (2005) 821–825.

[51]   T. Kushibiki, T. Hirasawa, S. Okawa, M. Ishihara, Blue laser irradiation generates intracellular reactive oxygen species in various types of cells., Photomed. Laser Surg. 31 (2013) 95–104.

[52]   T. Mosmann, Rapid colorimetric assay for cellular growth and survival: application to proliferation and cytotoxicity assays, J. Immunol. Methods. 65 (1983) 55–63.

[53]   Y.I. Svenskaya, H. Fattah, A.M. Zakharevich, D.A. Gorin, G.B. Sukhorukov, B.V. Parakhonskiy, Ultrasonically assisted fabrication of vaterite submicron-sized carriers, Adv. Powder Technol. (2016).

[54]   B. V. Parakhonskiy, A. Haase, R. Antolini, Sub-Micrometer Vaterite Containers: Synthesis, Substance Loading, and Release, Angew. Chem. Int. Ed. Engl. 51 (2012) 1195–1197.

[55]   C. Washington, Drug release from microdisperse systems: a critical review, Int. J. Pharm. 58 (1990) 1–12.

[56]   A.A. Antipov, G.B. Sukhorukov, E. Donath, H. Möhwald, Sustained Release Properties of Polyelectrolyte Multilayer Capsules, J. Phys. Chem. B. 105 (2001) 2281–2284.

[57]   A. Sergeeva, R. Sergeev, E. Lengert, A. Zakharevich, B. V. Parakhonskiy, D. Gorin, et al., Composite Magnetite and Protein Containing CaCO 3 Crystals. External Manipulation and Vaterite → Calcite Recrystallization-Mediated Release Performance, ACS Appl. Mater. Interfaces. 7 (2015) 21315–21325.

[58]   A. Lesniak, F. Fenaroli, M.P. Monopoli, C. Åberg, K.A. Dawson, A. Salvati, Effects of the Presence or Absence of a Protein Corona on Silica Nanoparticle Uptake and Impact on Cells, ACS Nano. 6 (2012) 5845–5857.

[59]   M. Lundqvist, J. Stigler, G. Elia, I. Lynch, T. Cedervall, K.A. Dawson, Nanoparticle size and surface properties determine the protein corona with possible implications for biological impacts., Proc. Natl. Acad. Sci. U. S. A. 105 (2008) 14265–70.

[60]   J.S. Gebauer, M. Malissek, S. Simon, S.K. Knauer, M. Maskos, R.H. Stauber, et al., Impact of the nanoparticle-protein corona on colloidal stability and protein structure., Langmuir. 28 (2012) 9673–9.

[61]   G. Caracciolo, The protein corona effect for targeted drug delivery, Bioinspired, Biomim. Nanobiomaterials. 2 (2012) 54–57.

[62]   A. Steff, M. Fortin, C. Arguin, P. Hugo, Detection of a decrease in green fluorescent protein fluorescence for the monitoring of cell death: An assay amenable to high-throughput screening, Cytometry. 243 (2001) 237–243.